Earth Surface Processes and Landforms
Earth Surf. Process. Landforms **29**, 105–114 (2004)
Published online in Wiley InterScience (www.interscience.wiley.com). DOI: 10.1002/esp.1021

LONGITUDINAL VELOCITY PATTERNS AND BED MORPHOLOGY INTERACTION IN A RILL

RAFAEL GIMÉNEZ[1]*, OLIVIER PLANCHON[2], NORBERT SILVERA[2] AND GERARD GOVERS[1]

[1] *Laboratory for Experimental Geomorphology, Catholic University of Leuven, Redingenstraat 16, 3000 Leuven, Belgium*
[2] *IRD – Institut de Recherche pour le Développement, BP 1386 Dakar, Senegal*

Received 22 November 2002; Revised 25 March 2003; Accepted 30 April 2003

ABSTRACT

Present-day understanding of rill dynamics is hampered by a lack of detailed data on velocity distributions in rills. The latter are difficult to collect with traditional techniques due to the very low water depths and the relatively high flow velocities in rills. The objectives of this paper were to investigate the feasibility of miniaturized acoustic Doppler velocimeter (mADV) measurements in rill flow and to explore longitudinal variations in flow velocities and their relationship with rill bed morphology. Detailed data on longitudinal flow velocity were required to achieve these objectives.

A 1·8 m long rill was formed freely in a flume at 5° slope and 0·001 $m^3 s^{-1}$ discharge. Rill topography was characterized by an alternation of steps and pools. The flume surface was then fixed to preserve rill roughness. A topographical scanning of the entire flume surface was made. Velocity was measured with a mADV along the rill, and at different depths. Flow depth in a longitudinal direction was also measured using an elevation gauge.

A strong relationship exists between rill topography and flow hydraulics. Over steps, flow was unidirectional and rapidly accelerating until a threshold Froude number (Fn) value between 1·3 and 1·7 was reached and a hydraulic jump occurred leading to the formation of a pool. In the pool, the flow pattern was multidirectional and complex. The flow was subcritical when leaving the pool and accelerated over the next step until the threshold Froude number value was again reached. Energy loss in the rill was concentrated in the pools, mainly due to the action of a hydraulic jump. This mechanism of energy dissipation appeared to be an essential factor in rill formation and bedform evolution. Copyright © 2004 John Wiley & Sons, Ltd.

KEY WORDS: velocity variation; rill flow velocity; step-pool bedforms

INTRODUCTION

Rills eroding cohesive materials are hydraulically different from alluvial rivers or large channels. Unlike rivers, rills are small, concentrated flow paths whose depth is of the order of only a few millimetres to centimetres and they have a relatively steep slope gradient. Also, rills evolve morphologically over much shorter timescales than rivers due to active bed erosion (Nearing *et al*., 1997; Lei *et al*., 1998).

Govers (1992) showed that the flow velocity in rills eroding loose, non-layered materials could be predicted from knowledge of discharge only, without a significant slope or soil effect. This finding has since then been confirmed by other authors such as Nearing *et al*. (1997, 1999), Takken *et al*. (1998), and Giménez and Govers (2001). Giménez and Govers (2001) were able to show that a feedback between bed morphology and flow hydraulics was a key factor in understanding this slope independence of flow velocity: bed roughness increased with slope gradient, thereby reducing flow velocity. Giménez and Govers also observed that the *average* Froude number (Fn) in eroding rills was roughly constant, as previously reported by Grant (1997) for a wide variety of streams with slopes exceeding 1 per cent and cohesionless bed material, and by Tinkler (1997) for the central thread of rockbed streams. Grant (1997) hypothesized that the near-critical, constant Fn observed in steep rivers is a consequence of a cyclical pattern of creation and destruction of bed forms, provided that there exists a flow with sufficient erosive power. This cyclical process is associated with cyclical changes of flow regimes (i.e. flow energy): from supercritical (i.e. $Fn > 1$) to subcritical (i.e. $Fn < 1$) along the whole stream, resulting in a near-critical average Fn.

* Correspondence to: R. Giménez, Laboratory for Experimental Geomorphology, Catholic University of Leuven, Redingenstraat 16, 3000 Leuven, Belgium. E-mail: rafael.gimenez@geo.kuleuven.ac.be

The mechanism responsible for the bed geometry–flow hydraulics feedback in rills cannot be entirely the same as the one reported by Grant because the rill bed consists of cohesive material and no mobile bedforms (Giménez and Govers, 2001). Therefore, Giménez and Govers (2001) proposed the following mechanism to explain their observations. Flow over a smooth bed on a steep slope is supercritical. Due to small local variations in flow depth, velocity and erosion resistance of the soil, local erosion occurs that leads to the formation of a small depression in the bed, which causes a hydraulic jump. Due to energy dissipation within the jump, additional local erosion occurs and a pool is formed. Within the pool, the flow is subcritical. The flow then accelerates in the downstream direction to become supercritical again and the whole process is repeated. This leads to a succession of pools, with subcritical flow, and steps, with supercritical flow. Giménez and Govers (2001) suggested that an increase in the slope reduces the distance needed to reach supercritical flow downstream from a pool. Consequently, the average number of pool–step systems per length unit will also increase with slope, but the average flow velocity will remain constant. It should be mentioned that the concept of relating rill initiation and evolution to the flow's Fn was already suggested by Savat and De Ploey (1982) who proposed that rills could only form when the flow exceeded a critical Fn value. However, they conceived this process as unidirectional rather than as bidirectional.

The hypothesis proposed by Giménez and Govers has not been tested yet. Conventional techniques used to measure flow velocities (e.g. dye tracing and surface tracing techniques with the aid of video recording) are not appropriate to obtain velocity data with the required accuracy and resolution. Recent developments in acoustic Doppler velocimeter (ADV) techniques make it possible to obtain detailed velocity measurements not only in relatively large channels (e.g. Robinson *et al*., 2000) but also in much narrower streams such as a rill. By using a miniaturized acoustic Doppler velocimeter (mADV) detailed velocity measurements are now possible in flows with a width of only 75 mm and a depth of only 20 mm.

The objectives of this study were to test the hypothesis of Gimenéz and Govers (2001) by investigating whether rill flow is indeed characterized by an alternation of sub- and supercritical flow reaches and, if so, how these variations are related to rill bed morphology. In order to achieve these objectives, detailed data on longitudinal variations in rill flow hydraulics were collected using an mADV probe.

MATERIALS AND METHODS

Set-up

The experiment was carried out in a flume 4·50 m long, 0·4 m wide and 0·45 m deep with a test section of 2·5 m length, which is described in detail by Giménez and Govers (2001). The lower 0·2 m of the flume was filled with a silt loam soil, which was manually compacted to simulate a subsoil: some characteristics of the soil material used are presented in Table I. The upper 0·25 m part of the test section was filled with the same soil but sieved at 20 mm in order to simulate fine seedbed conditions. The surface was smoothed with a rake, creating a 0·25–0·3 m wide and 50 mm deep longitudinal central depression with a flat bottom. The soil was then gently moistened to saturation and then left to drain to field capacity.

Rill formation and bed fixing

A rill was created in the topsoil of the test section in different stages as follows. The flume was set at a slope of 5°, and a discharge of 0·001 $m^3\ s^{-1}$ was applied for one minute. The average flow velocity was measured using

Table I. Soil characteristics

Grain-size classes (%)				
<2 μm	>50 μm	2–50 μm	D_{50} (μm)	Org. matter (%)
4·56	23·69	71·75	31·68	0·71

The granulometric analysis was done using laser diffractometry (Beuselinck *et al*., 1998).

a dye-tracing technique. Potassium permanganate solution was used as a dye, a small amount of which was injected 0·3–0·4 m upstream of the measurement section. Flow velocities were then measured by recording the travel time of the dye cloud over a distance of 1 m. The average travel time was taken as the mean of five measurements. The calculated velocities were multiplied by a correction factor of 0·94 as used by Govers (1992). The flume was then replaced in a horizontal position and a laser scanning of 18 cross-sections spaced 0·1 m apart was carried out. The system used for laser scanning is similar to the one described by Huang *et al*. (1988). A horizontal resolution of 1 mm was used. The vertical accuracy of the system is *c*. 0·1 mm. In order to obtain approximate longitudinal profiles of the rill at each stage of its development, the lowest point of each of the 18 cross-sections scanned after each experimental stage was determined: these points were then connected with a straight line to obtain an approximate longitudinal profile of the rill.

The entire operation described above was repeated seven times (i.e. the aforementioned discharge was applied during a total time of 7 min). During the entire operation, the downslope wall of the flume was lowered regularly in order to avoid significant deposition in the test section, which would affect rill formation. After 7 min, a well-defined rill was formed and flow conditions were at equilibrium, i.e. average flow velocity no longer changed significantly over time.

The flume surface was then fixed by spraying the entire surface with polyester resin diluted in acetone (1:5). Spraying was continued until resin infiltration stopped. Three applications of resin were carried out. Between applications, the flume surface was then left for 3–5 hours so that the resin could further infiltrate. After the final application, the resin was left to dry. Drying was accelerated using infrared lamps and a fan heater and resulted in the stabilization of the rill surface without affecting the rill bed topography. Velocities measured using dye tracing in the fixed rill were compared to those measured during the final stage of rill formation, using the same discharge and slope settings. The values that were obtained were very similar: $0{\cdot}45 \pm 0{\cdot}066$ m s^{-1} and $0{\cdot}48 \pm 0{\cdot}054$ m s^{-1}, respectively. This confirms that the resin application did not affect the rill bed roughness significantly.

After drying, the flume was placed in a horizontal position and a topographical scan of the central 1·8 m length of the test surface was made using a 1 mm horizontal interval in the transverse direction and a 2 mm horizontal interval in the longitudinal direction. A detailed longitudinal profile of the fixed rill was obtained from the DEM of the rill surface by selecting the lowest height value measured at every cross-section.

Experiments in the fixed rill

For the fixed rill experiments, the flume was replaced to the same slope used to create the rill (i.e. 5°) and the same discharge was applied (i.e. 0·001 m^3 s^{-1}). Detailed information on rill hydraulics was collected using various techniques.

Flow depth measurements. In order to obtain flow depths, the height of the water surface and of the lowest point of the rill bed was taken at 0·01 m intervals in the longitudinal direction using an elevation gauge with a precision of 0·2 mm that was mounted on a mobile frame on top of the flume. These measurements resulted in a rill bottom longitudinal profile, and a water surface profile. The rill bottom profile data were used to register the elevation gauge measurements with the laser scanner system of co-ordinates. The maximum water depth was then calculated by subtracting the laser bottom profile from the water surface profile.

mADV measurements. A miniaturized acoustic Doppler velocimeter (mADV; Figure 1) (SonTek, 1997) was used to obtain accurate average velocity measurements. The mADV head consists of a cylindrical transmitter at the centre, which is 13 mm in diameter, and two smaller receivers located at 37·5 mm at each side of the transmitter. The sampling volume is 5 mm^3 and is located 50 mm in front of the transmitter (Figure 1).

Measurements were carried out placing the mADV transmitter facing upstream so that the measurement head did not have an effect on the flow pattern within the sampling volume. The velocity determined at each sampling volume was calculated as an average of 100 readings, resulting in an accuracy of ±1 per cent. In order for the mADV to function properly the transmitter, the receivers, and the entire signal track from the transmitter to the sampling volume and back to the receivers must be fully submerged. In some places in the rill, complete submergence was not possible and hence no measurement could be carried out (Figure 2).

Two mADV measurements were taken every 10 mm along the central axis of the rill, refered to as *bottom* and *surface* velocity. The surface velocity measurement was taken *c*. 7 mm below the water surface,

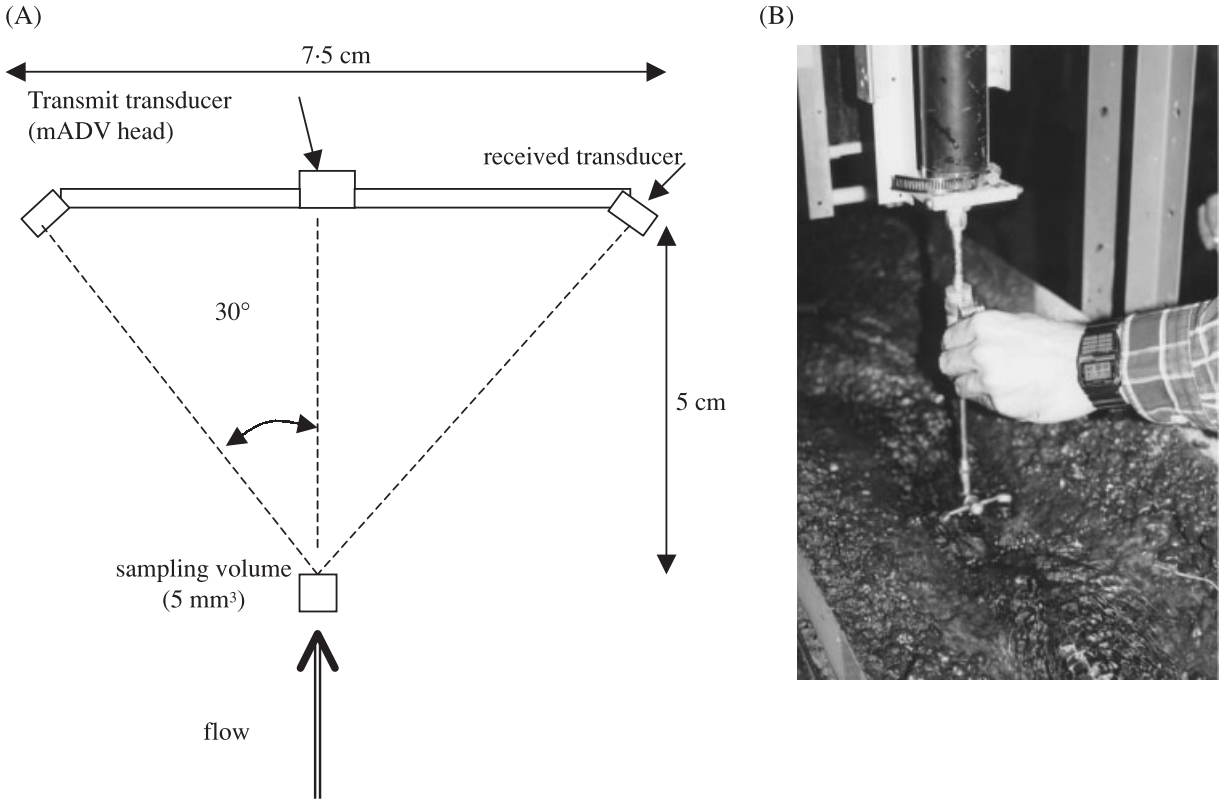

Figure 1. (A) Sketch of the mADV probe geometry; (B) photo of the mADV over the fixed rill. Flow is from front to back of the picture

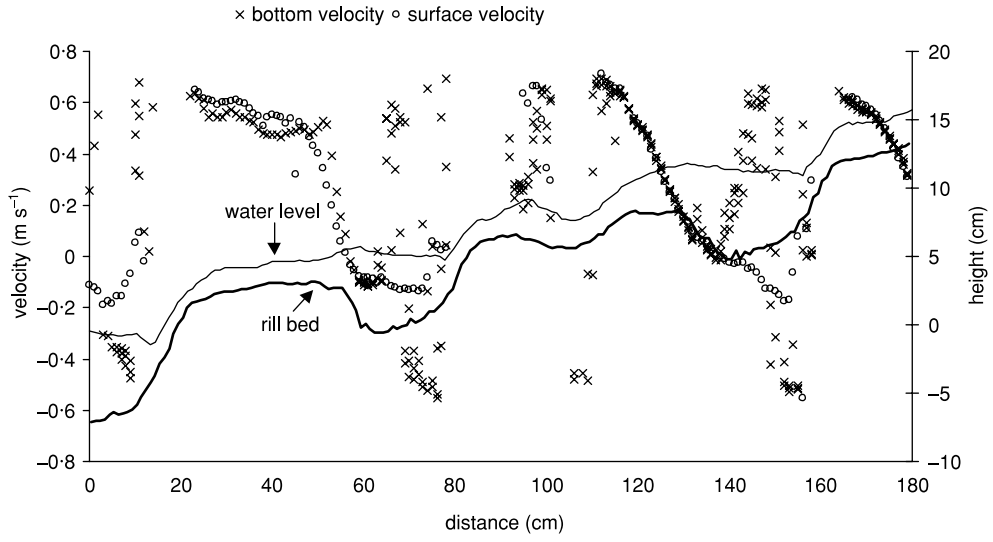

Figure 2. Longitudinal velocities along the rill. Positive velocity indicates forward flow, negative velocity indicates backward flow

which is the minimal depth at which the mADV can be operated. The bottom velocity was taken by placing the probe as deeply as possible in the rill. However, because there is a 50 mm distance between the transmitter and the sampling volume and the rill geometry varied significantly, the absolute height above the rill bottom at which measurements were taken was not constant. At some locations, the surface and bottom velocity

measurements had to be taken at almost the same depth due to the low water depth, resulting in almost identical values (Figure 2). The average of bottom and surface velocities was used in all further calculations (e.g. Fn determination).

RESULTS AND DISCUSSION

Rill bed morphology

The longitudinal height profile of the rill shows a succession of steps and pools (Figure 3): in the test section two well-defined pools were formed with approximately the same dimensions. Pool depth was *c*. 60 mm and pool length *c*. 320 mm. The pools were not symmetric: their downstream wall was steeper than their upstream wall. Between the two major pools, a small, embryonic pool was formed with a maximum depth of only 25 mm. All pools were separated by 'steps'. The slope gradient of the step surface was very close to the average slope gradient and each step was between 150 and 250 mm long. The average rill width was around 70–80 mm except in short V-shaped notches on the upstream pool brink where it suddenly decreased to 25–30 mm (see Figure 4).

Velocity pattern

Overall, consistent velocity measurements were obtained with the mADV. The data from the mADV show that the flow was unidirectional on the steps: average bottom and surface velocities were both positive. Within

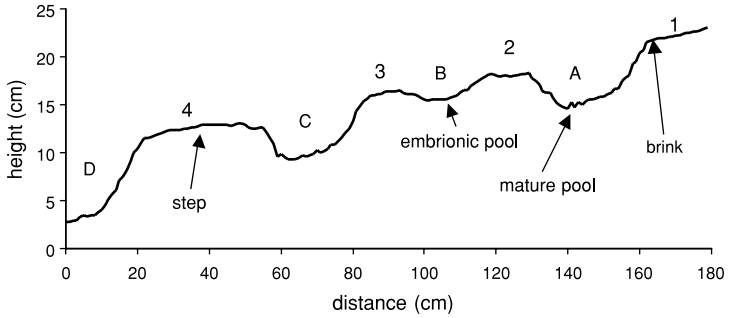

Figure 3. Longitudinal height profile of the rill where topographic features are indicated. Steps and pools are identified by numbers and letters, respectively: in the text, the different steps and pools are referred to by the same numbers and letters

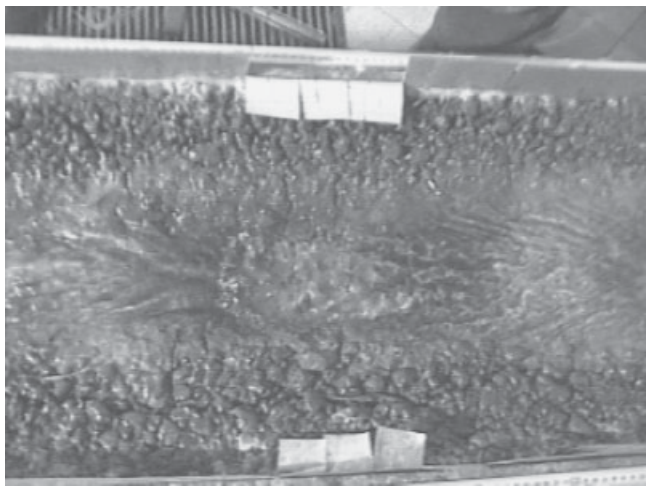

Figure 4. Plan view of a mature pool. A V-shaped notch is clearly observed upstream. Flow is from left to right. Flume is 40 cm wide

the pools the flow became multidirectional (i.e. water flowing downstream and upstream at different flow depths, Figure 2): the flow pattern within the pools was described and analysed in detail by O. Planchon *et al.* (work in preparation). It is worth pointing out that the multidirectional velocity pattern was not only observed in the mature pools, but also in the embryonic pool (Figure 2). Generally, the surface velocities were somewhat (<10 per cent) higher than the corresponding bottom velocities (Figure 2): the small difference between bottom and surface velocity indicates that the vertical velocity gradient on the steps was quite low. The flow over the steps accelerated from the exit of pools, where measured velocities were as low as *c.* $0{\cdot}20 \pm 0{\cdot}06$ m s^{-1} up to immediately before the brink of the next pool downstream, where it reached a more or less constant value of *c.* $0{\cdot}70 \pm 0{\cdot}06$ m s^{-1} (Figure 2).

Froude number pattern

The Froude number, Fn, for open channel flow is defined as:

$$\mathrm{Fn} = \frac{v}{\sqrt{gd}} \tag{1}$$

where v is flow velocity, g is gravitational acceleration and d is flow depth.

Fn calculations in this study were based on *local* values of velocity and flow depth. Consequently, Fn values were assessed only for a narrow vertical panel of water along the central flow thread. Strictly, this is the only correct approach to calculate the Fn in flows with important lateral variations (Ligget, 1993; Tinkler, 1997).

Meaningful values of Fn could only be calculated in the zones where flow is unidirectional, i.e. at the pool exits and on the steps. The calculation of Fn in the pools was considered to be meaningless due to the occurrence of multidirectional flow.

Froude numbers increased from the pool exit, where flow was subcritical, towards the brink of the downstream pool (Figure 5). At the onset of the brink, Fn reached values between 1·3 and 1·7. A similar pattern was observed in both the major pools and in the embryonic pool: the flow was supercritical when entering the pool and subcritical when leaving it (Figure 5). Fn could not be calculated at the chute (i.e. the sloping, narrow rill section at the entrance of the pool) as no velocity measurements were available because of the shallow flow depths and the small rill width.

Thus, our measurements show that there were important longitudinal variations of flow velocity and Fn along the rill. However, the pattern did not consist of a simple alternation of supercritical and subcritical flow zones, as hypothesized by Giménez and Govers (2001). At the pool exit, flow was indeed unidirectional and subcritical. The flow then accelerated over the step until the Fn reached values well above 1. A hydraulic jump occurred when the flow entered the pool. In the pools, flow was not simply subcritical, but displays a rather complex, multidirectional pattern.

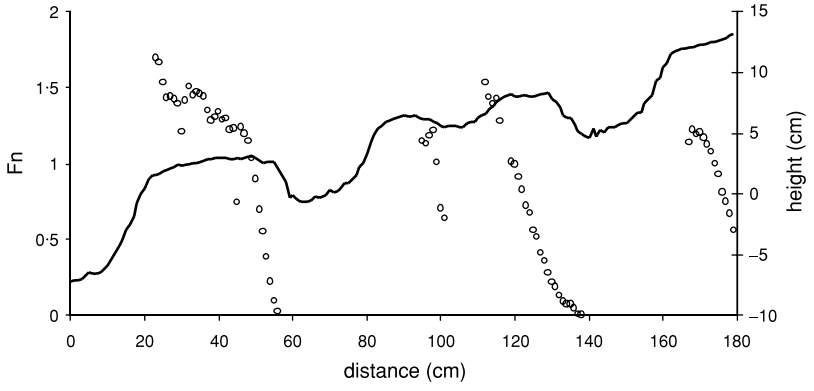

Figure 5. Local Froude number pattern along the rill. Values within the pools are not considered (see text for explanation)

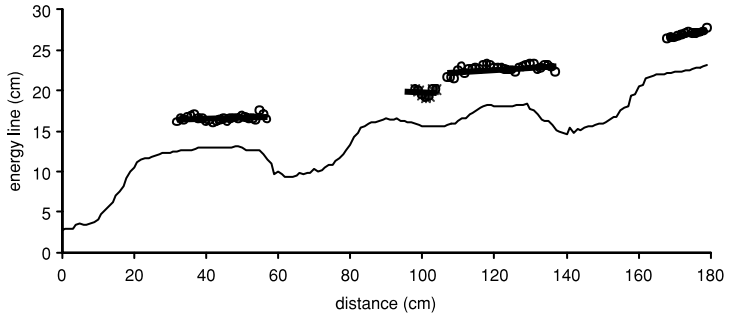

Figure 6. Total energy of the flow at different sections along the rill with reference to a datum line. Lines were obtained by regression

Energy gradient along the rill

The total energy of a streamline, H, can be estimated as (e.g. Chow, 1985, p. 39):

$$H = z + d + \frac{v^2}{2g} \tag{2}$$

where z is elevation of a certain defined point above a datum plane, d is depth of this point below the water surface (i.e. pressure head), v is velocity of the flow in the streamline passing through the point and g is gravitational acceleration.

Ignoring minor disturbances due to turbulence, H can be estimated only on the steps and at the pool exits, where the streamlines have neither appreciable curvature nor divergence, i.e. hydrostatic pressure distribution can be assumed. However, H cannot be estimated in the pools where the pressure gradient is not hydrostatic due to the high turbulence of flow (Chow, 1985, p. 30). It can be seen that the energy line is almost horizontal from the pool exit to the step brink (Figure 6): the decrease on potential energy (i.e. z) is roughly counteracted by the increase in velocity (i.e. kinetic energy). Within the pools important energy dissipation took place. The low gradient of the energy line on the steps, combined with the low flow depths implies that the shear stress in these areas was quite low.

Energy dissipation in pools

A pool has a morphological structure which is to some extent similar to a *drop structure* as defined elsewhere (Chanson, 1999, p. 355). Energy dissipation within a drop structure is mainly a consequence of two mechanisms: part of the flow energy is dissipated by the chute impact (i.e. chute impingement) and then the residual energy is dissipated by a hydraulic jump located downstream of the chute toe. For a *chute flow* situation (i.e. a succession of drop structures; Chanson, 1999, p. 362), the relative energy loss on the cascade up to the hydraulic jump, Φ_{cas}, can be estimated as follows (Chanson, 1999, p. 363):

$$\Phi_{cas} = 1 - \Phi_j = 1 - \frac{0{\cdot}54\left(\frac{dc}{\Delta z}\right)^{0{\cdot}275} + 1{\cdot}715\left(\frac{dc}{\Delta z}\right)^{-0{\cdot}55}}{1{\cdot}5 + \frac{\Delta z}{dc}} \tag{3}$$

where:

$$\Phi_{cas} = \frac{\Delta H_{cas}}{H_b}$$

$$\Phi_j = \frac{\Delta H_j}{H_b}$$

Table II. Hydraulic conditions at the four pools

Parameters	Pool*			
	A	B	C	D
d_b	2·51	2·03	1·6	1·5
dc	3·51	2·84	2·23	2·1
Δz	5·2	2·24	4·66	5·43
H_b	9·82	6·86	8·5	9·0
Φ_{cas}	0·12	0·10	0·16	0·19
Φ_j	0·88	0·90	0·84	0·81

d_b = flow depth at the brink; $dc = d_b/0{\cdot}715$; Δz = maximum height of the pool upstream wall; H_b = (relative) total energy at the brink; Φ_{cas} = (relative) total energy dissipated in a pool up to the chute toe; Φ_j = (relative) total energy dissipated by the hydraulic jump downstream.

* For location of the pools, see Figure 3.

H_b is maximum head available at the brink of the cascade (with the datum located at the dam toe), ΔH_{cas} is total head loss along the *drop cascade* (*~pool chute*), ΔH_j is total head loss along the hydraulic jump downstream, Φ_j is (relative) residual energy at the chute toe dissipated by the hydraulic jump and Δz is *dam crest elevation* above the downstream toe (*~height of the upstream wall of a pool*).

H_b and dc can be calculated empirically as follows:

$$H_b = \Delta z + 1{\cdot}5\,dc \qquad \text{(Chanson, 2001, p. 100)} \tag{4}$$

$$dc = 1{\cdot}4\,d_b \qquad \text{(Chanson, 1999, p. 358)} \tag{5}$$

where d_b is flow depth over the brink of the cascade.

It is obvious that rill pools are not entirely identical to a drop structure. The main differences are that the pool walls are not vertical and the pool bed is not entirely horizontal. Using Equation 3 to estimate energy losses due to chute impact will therefore lead to an overestimation of Φ_{cas} as energy dissipation due to chute impingement will be reduced by the lower angle of impact of the chute flow in a rill pool compared to a drop structure. Using Equation 3, it is estimated that only 10–20 per cent of total energy dissipation in the pool can be attributed to chute impingement (Table II). As this estimate is almost certainly too high, it can be safely stated that energy dissipation in the pools is mainly due to the occurrence of a hydraulic jump. This implies that energy dissipation is concentrated in the central area of the pool, which may explain why during rill formation pools mainly expanded by deepening and to a much lesser extent by retreat of the upstream pool wall (Figure 7).

Interestingly, even in the embryonic pool with a depth of only 25 mm a supercritical–subcritical transition was evident: the threshold Fn value at which the transition occurred was very similar to the maximum values of Fn measured upstream of the brink of the mature pools (1·3–1·7). Thus, minor bed irregularities can induce a hydraulic jump if Fn is sufficiently high. The hydraulic jump will then lead to the formation of a deeper pool with which a hydraulic chute will be associated.

The experiment presented in this paper allowed us to analyse the longitudinal variations in flow velocities in a rill in detail: our results show that flow in the test rill consists of an alternation of supercritical and complex/subcritical reaches. This alternation was closely coupled to bed morphology. However, as experiments were hitherto carried out on a single slope and with a single discharge only, no definite answer can be given to the question as to why flow velocities in rills are independent of slope gradient. However, some observations can be made. It is known that in eroding rills a constant average Fn is maintained (Giménez and Govers, 2001). On the other hand, our present results show that, when the local Fn exceeds a constant supercritical value a hydraulic jump is generated leading to the formation of a pool and a chute. In our experiment, we found a rather constant critical Fn value between 1·3 and 1·7. The question may be asked as to why a hydraulic jump does not occur when the Froude number exceeds a value of 1·0. Chow (1985, p. 395) and Chanson (1999, p. 63) state that a

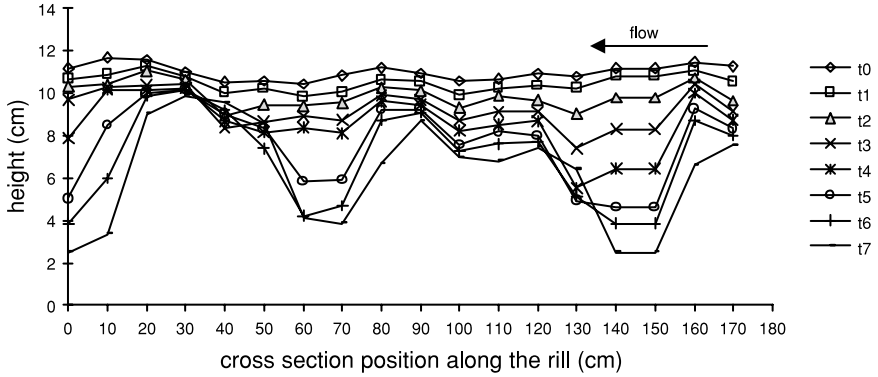

Figure 7. Longitudinal height evolution of the rill along time. t1–t7 are periods of 1 minute in increasing order; t0 is soil surface before the erosion process started

clear hydraulic jump, with significant energy losses, will only occur when Fn exceeds 1·7. For lower values of Fn, undular flow occurs, with negligible energy losses. It should be kept in mind though that the threshold value at which a hydraulic jump starts to form is not constant: it depends on local bed morphology and slope characteristics (Chanson, 2000).

In order to reach a given threshold Fn value downstream of a hydraulic jump the flow needs to accelerate over a step. Considering that the flow width and hence the unit discharge in a rill are independent of slope gradient (Gilley *et al*., 1990; Giménez and Govers, 2001), the step length necessary to reach this threshold value will decrease with increasing slope gradient. Hence, the frequency of step–pool alternations should increase with increasing slope gradient. This is in agreement with observations that roughness frequency of rill beds increases with slope gradient (Giménez and Govers, 2001). However, the longitudinally averaged value of Fn and hence the average flow velocity will not be strongly affected by this increased frequency of alternation of supercritical and complex/subcritical flow. On the other hand, if a constant Fn is maintained flow velocity can increase with discharge as flow width and flow depth also increase with discharge (Giménez and Govers, 2001).

CONCLUSIONS

Our results show that present-day mADV probes can be successfully used to study longitudinal variations in flow velocity in a rill in detail. In our experiment, rill topography was characterized by an alternation of steps and pools which was strongly related to the flow hydraulics. Over steps, flow was unidirectional and rapidly accelerating until a threshold Fn value between 1·3 and 1·7 was reached and a hydraulic jump occurred leading to the formation of a pool. In the pool, the flow pattern was multidirectional and complex. The flow was subcritical when leaving the pool and accelerated over the next step until the threshold Fn value was again reached.

The alternation of complex subcritical flow and unidirectional supercritical flow leads to an average Fn that is near 1. On steeper slopes, it may be expected that the alternation of different flow regimes and associated bedforms will occur with a higher frequency: this will lead to an increase of bed roughness but not to an increase of flow velocity, provided that the threshold value of Fn is constant. Comparison of incipient and mature pools shows that most important elements of longitudinal variation in flow structure, such as flow acceleration and the presence of a hydraulic jump, are always present.

The data presented in this paper support the hypothesis put forward in an earlier paper that the slope independence of flow velocity in eroding rills is due to an alternation of supercritical and subcritical flow sections, resulting in an average constant Froude number and the average flow velocity being independent of slope. However, rill pools are characterized by a complex multidirectional flow pattern. Experiments using different slopes, discharges and perhaps soil types are necessary to investigate whether the pattern we described is indeed general.

Energy loss in the rill is concentrated in the pools. This energy loss is mainly due to the action of a hydraulic jump and to a much lesser extent to chute impingement. This mechanism of energy dissipation is an essential element in rill formation and bedform evolution. Another issue that warrants further attention in future experiments is the effect that the presence of sediment might have on rill hydraulics.

REFERENCES

Beuselinck L, Govers G, Poesen J, Degraer G, Froyen L. 1998. Grain-size analysis by laser diffractometry: comparison with the sieve-pipette method. *Catena* **32**: 193–208.

Chanson H. 1999. *The Hydraulics of Open Channel Flow. An Introduction*. John Wiley & Sons Inc: New York.

Chanson H. 2000. Boundary shear stress measurements in undular flows: application to standing wave bed forms. *Water Resources Research* **36**(10): 3063–3076.

Chanson H. 2001. *The Hydraulics of Stepped Chutes and Spillways*. Balkema: Lisse, The Netherlands.

Chow VT 1985. *Open-Channel Hydraulics*. McGraw-Hill International: New York.

Gilley JE, Kottwitz ER, Wieman GA. 1990. Hydraulic characteristics of rills. *Transactions of the ASAE* **33**(6): 1900–1906.

Giménez R, Govers G. 2001. Interaction between bed roughness and flow hydraulics in eroding rills. *Water Resources Research* **37**(3): 791–799.

Govers G. 1992. Relationship between discharge, velocity and flow area for rills eroding loose, non-layered materials. *Earth Surface Processes and Landforms* **17**: 515–528.

Grant GE. 1997. Critical flow constrains flow hydraulics in mobile-bed streams: a new hypothesis. *Water Resources Research* **33**(2): 349–358.

Huang C, White EG, Thwaite EG, Bendeli A. 1988. A noncontact laser system for measuring soil surface topography. *Soil Science Society of America Journal* **52**: 350–355.

Lei TW, Nearing MA, Haghighi K, Bralts VF. 1998. Rill erosion and morphological evolution: a simulation model. *Water Resources Research* **34**(11): 3157–3168.

Ligget JA. 1993. Critical depth, velocity profiles, and averaging. *Journal of Irrigation and Drainage Engineering*. **119**: 416–422.

Nearing MA, Norton LD, Bulgakov DA, Larionov GA. 1997. Hydraulics and erosion in eroding rills. *Water Resources Research* **33**(4): 865–876.

Nearing MA, Simanton JR, Norton LD, Bulygin SJ, Stone J. 1999. Soil erosion by surface water flow on a stony, semiarid hillslope. *Earth Surface Processes and Landforms* **24**(8): 677–686.

Robinson KM, Cook KR, Hanson GJ. 2000. Velocity field measurements at an overfall. *Transactions of the ASAE* **43**(3): 665–670.

Savat J, De Ploey J. 1982. Sheetwash and rill development by surface flow. In *Badland Geomorphology and Piping*, Bryan R, Yair A (eds). Geo Books: Norwich; 113–126.

SonTek. 1997. *Acoustic Doppler Velocimeter Operation Manual, version 4.0*. SonTek: San Diego.

Takken I, Govers G, Ciesiolka CAA, Silburn DM, Loch RJ. 1998. Factors influencing the velocity-discharge relationship in rills. *IAHS Publication* **249**: 63–69.

Tinkler KJ. 1997. Critical flow in rockbed streams with estimated values for Manning's n. *Geomorphology* **20**(1–2): 147–164.

